Development/Plasticity/Repair

Cdk5-Dependent Mst3 Phosphorylation and Activity Regulate Neuronal Migration through RhoA Inhibition

Jing Tang,[1,2,3] Jacque P.K. Ip,[1,2,3] Tao Ye,[1,2,3] Yu-Pong Ng,[1,2,3] Wing-Ho Yung,[4] Zhenguo Wu,[1,2,3] Weiqun Fang,[1,2,3] Amy K.Y. Fu,[1,2,3] and Nancy Y. Ip[1,2,3]

[1]Division of Life Science, [2]State Key Laboratory of Molecular Neuroscience, and [3]Molecular Neuroscience Center, The Hong Kong University of Science and Technology, Clear Water Bay, Kowloon, Hong Kong, China, and [4]School of Biomedical Sciences, The Chinese University of Hong Kong, Shatin, NT, Hong Kong, China

The radial migration of newborn neurons is critical for the lamination of the cerebral cortex. Proper neuronal migration requires precise and rapid reorganization of the actin and microtubule cytoskeleton. However, the underlying signaling mechanisms controlling cytoskeletal reorganization are not well understood. Here, we show that Mst3, a serine/threonine kinase highly expressed in the developing mouse brain, is essential for radial neuronal migration and final neuronal positioning in the developing mouse neocortex. Mst3 silencing by *in utero* electroporation perturbed the multipolar-to-bipolar transition of migrating neurons and significantly retards radial migration. Although the kinase activity of Mst3 is essential for its functions in neuronal morphogenesis and migration, it is regulated via its phosphorylation at Ser79 by a serine/threonine kinase, cyclin-dependent kinase 5 (Cdk5). Our results show that Mst3 regulates neuronal migration through modulating the activity of RhoA, a Rho-GTPase critical for actin cytoskeletal reorganization. Mst3 phosphorylates RhoA at Ser26, thereby negatively regulating the GTPase activity of RhoA. Importantly, RhoA knockdown successfully rescues neuronal migration defect in Mst3-knockdown cortices. Our findings collectively suggest that Cdk5–Mst3 signaling regulates neuronal migration via RhoA-dependent actin dynamics.

Key words: **actin; cyclin-dependent kinase; neuronal migration; Rho-GTPase**

Introduction

Cortical functions require precise wiring of distinct laminar-specific neural circuitry (Douglas and Martin, 2004). Radial migration, in which newborn neurons radially migrate to their final locations in the cerebral cortex, is one of the key steps that determines cortical function (Sidman and Rakic, 1973; Guerrini et al., 2008) and disruptions to neuronal migration are frequently associated with cortical malformation disorders and neuropsychiatric diseases such as schizophrenia and autism (Gleeson and Walsh, 2000; Deutsch et al., 2010; Singh et al., 2010; Valiente and Marin, 2010; Wegiel et al., 2010). Multiple cellular events are precisely regulated and coordinated to ensure proper neuronal migration (Bielas et al., 2004; Ayala et al., 2007; Creppe et al., 2009; Guerrier et al., 2009). A transient multipolar migration occurs in the lower intermediate zone (Nadarajah and Parnavelas, 2002; LoTurco and Bai, 2006). The subsequent multi-to-bipolar transition allows the migrating neurons to acquire a single leading process and initiate the glia-guided locomotion (Nadarajah and Parnavelas, 2002; LoTurco and Bai, 2006). Impairment of the transition leads to the inability of migrating neurons entering the cortical plate and eventually causes severe migration defects such as heterotopia (Ayala et al., 2007). However, the molecular mechanisms underlying the regulation of multipolar-to-bipolar transition remain unclear.

Emerging evidence suggests that protein kinases are important regulators for neuronal migration via the modulation of the cytoskeletal dynamics (Kawauchi and Hoshino, 2008; Su and Tsai, 2011). For example, cyclin-dependent kinase 5 (Cdk5), a serine/threonine kinase, plays a key role in neuronal migration by phosphorylating and regulating cytoskeletal regulators such as the actin-binding protein cofilin and the microtubule-binding protein doublecortin (Tanaka et al., 2004; Kawauchi et al., 2006). Cdk5 also triggers the activation of various kinase cascades to coordinate various cellular events during neuronal migration, such as the phosphorylation of focal adhesion kinase and p21-activated kinase (Rashid et al., 2001; Xie et al., 2003). Nonetheless, it remains unclear how these kinases are precisely regulated during neuronal migration.

Mammalian Ste20-like kinase (Mst), a serine/threonine kinase family member originally identified as a regulator of cell

Received Dec. 30, 2013; revised April 8, 2014; accepted April 18, 2014.

Author contributions: J.T., J.P.K.I., T.Y., W.-H.Y., A.K.Y.F., and N.Y.I. designed research; J.T., J.P.K.I., T.Y., W.-H.Y., and W.F. performed research; Y.-P.N., Z.W., and N.Y.I. contributed unpublished reagents/analytic tools; J.T., J.P.K.I., T.Y., W.-H.Y., W.F., A.K.Y.F., and N.Y.I. analyzed data; J.T., J.P.K.I., A.K.Y.F., and N.Y.I. wrote the paper.

The authors declare no competing financial interests.

This work was supported by the Research Grants Council of Hong Kong SAR (Grants HKUST660810, HKUST660711, HKUST661111, HKUST661212, and HKUST660213), the National Key Basic Research Program of China (Grant 2013CB530900), the Theme-based Research Scheme of the University Grants Committee (Grant T13-607/12-R), the Innovation and Technology Fund for State Key Laboratory (Grant ITCPT/17-9), the Shenzhen Peacock Plan, and the S.H. Ho Foundation. We thank Cara Kwong, Busma Butt, Wanting Zhong, and William Chau for excellent technical assistance; other members of the Ip laboratory, in particular Dr. Lei Shi, for helpful discussions; and Xuemin Zhang and Weihua Li (National Center of Biomedical Analysis) for providing help in mass spectrometry analysis.

Correspondence should be addressed to either Amy K.Y. Fu or Nancy Y. Ip, Division of Life Science, The Hong Kong University of Science and Technology, Clear Water Bay, Hong Kong, China, E-mail: boip@ust.hk or boamy@ust.hk.

DOI:10.1523/JNEUROSCI.5449-13.2014

 0270-6474/14/347425-12$15.00/0

death, was recently reported to play important roles in the regulation of neuronal functions (Lehtinen et al., 2006; Ling et al., 2008; Xiao et al., 2011). The *Drosophila* homolog of Mst, Hpo, regulates dendrite development (Emoto et al., 2006), whereas an isoform of Mst3 has been implicated in axon outgrowth and regeneration (Irwin et al., 2006; Lorber et al., 2009). However, the precise roles of Mst3 in the developing CNS and its molecular regulation are unclear.

In this study, we report an essential role of Mst3 in neuronal positioning. *In utero* silencing of Mst3 disrupts the multipolar-to-bipolar transition and significantly retards radial migration. Moreover, we found that the kinase activity of Mst3 is regulated via the Cdk5-dependent phosphorylation at Ser79. Interestingly, Mst3 regulates neuronal migration through modulating the activity of RhoA, a Rho-GTPase critical for actin reorganization (Hall, 1994). RhoA knockdown restored normal neuronal migration in Mst3-knockdown cortices. Our findings collectively suggest that Cdk5–Mst3 signaling regulates neuronal migration via RhoA-dependent actin dynamics.

Materials and Methods

Constructs. FLAG-tagged full-length mouse Mst3 plasmids were constructed by cloning the cDNAs of Mst3 wild-type (WT) or its kinase-dead mutant into the pCDNA3 vectors. For gene knockdown by RNA interference (RNAi), pSUPER vector-based small hairpin RNAs (shRNAs) of Mst3, Mst3-scramble, and RhoA were constructed. The shRNA target sense sequences for Mst3, Mst3-scramble, and RhoA were 5′-GGAC TTGATTATCTACACT-3′, 5′-GTCATAATCGCATGTCTTA-3′, and 5′-GAAAGCAGGTAGAATTGGC-3′, respectively (Conery et al., 2010). RNAi-resistant Mst3 expression constructs were generated by introducing three silent mutations into the cDNA sequence targeted by Mst3 shRNA; the primer sequence was 5′-CGAGAAATTCTGAAAGGACT AGACTACTTACATTCGGAGAAGAAAATTC-3′ and the amino acids were not changed.

Antibodies. Antibodies against Mst3 (sc-135993), HA (sc-805), Cdk5 (DC17), p35 (C-19), and RhoA (sc-418) were purchased from Santa Cruz Biotechnology. Anti-Mst3 (3723S) and anti-phospho-(Ser) CDKs substrate (2324S) were from Cell Signaling Technology. Antibodies against GAPDH (AM4300), Mst3 (EP1468Y), and phospho-serine (AB1603) were from Ambion, Epitomics, and Millipore, respectively. Anti-FLAG (M2), anti-Tuj1 (T3952), anti-CS-56 (C8035), and anti-β-actin (A5316) were from Sigma. Anti-phospho-Ser79-Mst3 antibody was raised in a rabbit immunized with a synthetic peptide (CVLSQCDS(P) PYVTKYY; Biosynthesis) and purified using the SulfoLink Kit (Thermo). His-RhoA protein (RH01) was from Cytoskeleton and the Mst3 recombinant protein (PV3650) was from Invitrogen.

Experimental animals and in utero *electroporation*. *Cdk5*-knock-out mice were provided by A.B. Kulkarni (National Institutes of Health). *In utero* electroporation was performed as described previously (Ip et al., 2012). ICR mice of either sex were used for *in utero* electroporation at indicated ages. For knockdown experiments, the mice were coinjected with pCAG2IG expressing GFP and pSUPER plasmid, scramble shRNA, or Mst3 shRNA in a 1:2 ratio on embryonic day 14 (E14) and brains were collected on E17, E18, or postnatal day 2 (P2) or P5. For rescue experiments, Mst3 shRNA was mixed with pCAG2IG expressing different rescue constructs (in a 2:3 ratio) and coinjected into the mice. For the RhoA double-knockdown experiment, GFP, Mst3 shRNA, and RhoA shRNA were mixed (2:2:0.5) and coinjected into the mouse brains.

Primary neuron cultures, *transfection*, *and treatment*. Primary cortical neuron cultures were prepared from E18 rats and maintained as described previously (Fu et al., 2007). Nucleofector (Amaxa Biosystems) or Lipofectamine 2000 (Invitrogen) was used to deliver plasmids into cultured neurons. For pharmacological treatment, cortical neurons (1×10^7 cells per plate) were treated with 200 nM 6-bromoindirubin-3′-acetoxime, 10 μM roscovitine, 10 μM SP600125, 100 nM UO126 (Calbiochem), or 20 μM H89 (Sigma) for 1 h. Neurons at 4 d *in vitro* (DIV) were subjected to immunoprecipitation and Western blot analysis.

Cell cultures, *transfection*, *protein extraction*, *and immunoprecipitation*. HEK293T cells were cultured in DMEM with 10% heat-inactivated fetal bovine serum, 50 units/ml penicillin, and 100 μg/ml streptomycin at 37°C in a 5% CO_2 humidified atmosphere. Lipofectamine and Plus transfection reagents were from Invitrogen. Protein extraction and immunoprecipitation were performed as described previously (Fang et al., 2011). In brief, 1–2 mg of protein lysate was incubated with 2 μg of antibody at 4°C for 3 h with end-to-end rotation; the antibody was subsequently pulled down by protein G-Sepharose beads (GE Healthcare) for 1 h.

In vitro *phosphorylation assay*. The *in vitro* phosphorylation assay was performed as described previously (Fu et al., 2007). In brief, recombinant kinases or immunoprecipitated kinases were incubated in kinase buffer [20 mM MOPS; 3-(*N*-morpholino)-propanesulfonic acid, pH 7.4, 15 mM $MgCl_2$, 20 mM $MnCl_2$, and 100 μM ATP] containing 1–2 μCi [γ-^{32}P] ATP with 8 μg of histone H1 protein or immunoprecipitated proteins at 30°C for 30 min with shaking at 900 rpm. The phosphorylated protein was subsequently separated using SDS-PAGE and visualized by autoradiography. In particular, to examine the activity of Mst3 in the mouse brain, equal amounts of brain lysates at the indicated stages were immunoprecipitated with anti-Mst3 antibody, followed by incubation with recombinant histone H1 protein in kinase reaction buffer for *in vitro* phosphorylation assay. For identification of the Cdk5 phosphorylation site on Mst3, HEK293T cells expressing WT or one of three phospho-deficient mutants of Mst3 at putative Cdk5 phosphorylation sites were pulled down by anti-FLAG antibody, incubated with or without Cdk5/p35 complex, and subjected to an *in vitro* kinase assay.

Filamentous/globular actin ratio and growth cone collapse assay. For determining the ratio of filamentous actin (F-actin) and globular actin (G-actin) (Meller et al., 2008), cortical neurons were transfected with pSUPER or Mst3 shRNA by nucleofection at 0 DIV. Four days after transfection, the neurons were homogenized in F-actin stabilization buffer and ultracentrifuged to separate F-actin (pellet fraction) and G-actin (supernatant fraction) pools. The two fractions were separated by SDS-PAGE and actin was quantified by Western blotting using anti-actin antibody. Growth cone collapse was performed as described previously (Shi et al., 2007). In brief, cultured cortical neurons from E14 ICR mice were transfected with GFP and pSUPER or Mst3 shRNA by nucleofection. At 4 h after transfection, the neurons were treated with 10 μM ROCK inhibitor (RI: Y27632) for 20 h and subsequently fixed. The fixed neurons were stained with anti-GFP, anti-Tuj1 antibodies, and fluorescently labeled phalloidin.

Electrophysiology. *In utero* electroporation was performed at E14. Electrophysiological recordings were performed on cortical slices prepared at P15–P20. Briefly, mice of either sex were anesthetized and brains were rapidly dissected in ice-chilled artificial CSF (ACSF) containing the following (in mM): 126 NaCl, 3.5 KCl, 2 $CaCl_2$, 1.3 $MgCl_2$, 25 $NaHCO_3$, 1.2 $NaHPO_4$, and 10 glucose at 95% O_2, 5% CO_2, pH 7.4. Coronal brain slices (250 μm) prepared using a vibratome were kept in oxygenated ACSF at room temperature for 1 h before recordings. The slices were transferred to a chamber mounted onto a fixed-stage upright microscope (BX51WI; Olympus) equipped with an epifluorescent attachment and superfused with ACSF at physiological temperature. Conventional whole-cell recordings were made from target cortical neurons, including GFP^+ neurons, aided by differential interference contrast optics. Microelectrodes had a resistance of 6–8 MΩ. All electrophysiological data were digitized by the Digidata pClamp system and analyzed with MiniAnalysis (Synaptosoft).

Quantification and statistical analysis. For the morphological analysis of dendrite length at P5, *z*-series confocal images of cortical sections were collected at 1 μm steps with 10 optical sections in Fluoview (Olympus). In the stacked images, an apical dendrite was traced manually and the dendrite length was measured using ImageJ software. Quantification results are showed as mean ± SEM. Statistical significance was determined using unpaired Student's *t* test.

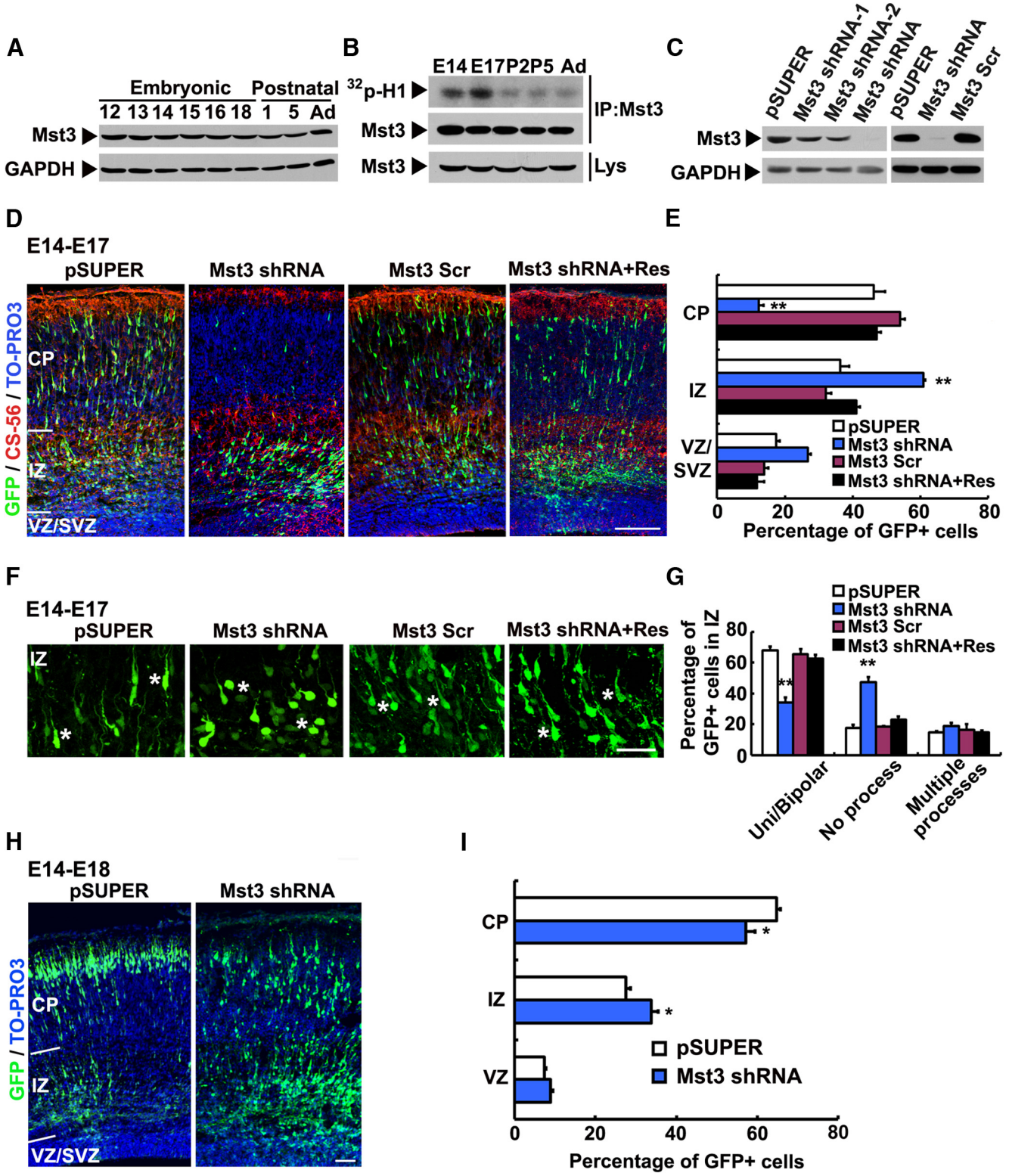

Figure 1. Mst3 is important for radial migration in the mouse cerebral cortex. ***A***, Developmental expression of Mst3 protein in the mouse brain. Whole-brain lysates at various developmental stages (E12 to adult) were subjected to Western blotting for Mst3 with GAPDH as a loading control. ***B***, Developmental regulation of Mst3 activity in the mouse brain. Whole-brain lysates at different developmental stages were subjected to a kinase activity assay using histone H1 as the substrate. ***C***, Knockdown of endogenous Mst3 expression in neurons by pSUPER-Mst3 shRNA constructs. Cultured cortical neurons at 0 DIV were transfected with one of three different pSUPER-Mst3 shRNAs or scrambled shRNA. Protein lysates were collected at 4 DIV and subjected to Western blotting for Mst3 and GAPDH as a control. ***D–I***, Mst3 knockdown arrested migrating cortical neurons in the intermediate zone (IZ) in the early stage. E14 mouse embryos were electroporated with GFP expression construct and pSUPER, Mst3 shRNA, or Mst3 scramble shRNA (Mst3 Scr) by *in utero* electroporation. Mouse brain sections were collected at E17 (***D–G***) and E18 (***H***, ***I***). ***D***, Representative images stained for GFP (green) and CS-56 (subplate marker, red), and counterstained with TO-PRO-3 (nuclear marker, blue). SVZ, Subventricular zone; VZ, ventricular zone; CP, cortical plate. Scale bar, 100 μm. ***E***, Quantification of the distribution of GFP$^+$ neurons in ***D***. $^{**}p < 0.01$ versus pSUPER, $n = 3$ experiments, Student's *t* test, mean $\pm$ SEM. More than 500 GFP$^+$ neurons from six brains were analyzed in each group. ***F***, Mst3 knockdown resulted in impaired morphology of migrating neurons in the IZ. Asterisks indicate representative neurons with unipolar/bipolar morphology in the pSUPER, Mst3 Scr, and Mst3-WT Res groups in contrast to no process morphology in Mst3 shRNA group. Scale bar, 25 μm. ***G***, Quantification of the (*Figure legend continues.*)

Results

Mst3 regulates radial migration and neuronal morphology in the mouse cerebral cortex

To investigate the role of Mst3 in the brain, we first examined its expression profile in the mouse brain during development. Although Mst3 protein was prominently expressed in the cerebral cortex from early embryonic stages through adulthood (Fig. 1*A*), its kinase activity was particularly robust from E14–E17, when extensive active neuronal migration occurs (Fig. 1*B*). Three Mst3 shRNAs were generated to study the function of Mst3; one of them in particular efficiently depleted the expression of endogenous Mst3 in cultured cortical neurons, whereas scrambled shRNA did not reduce Mst3 expression levels (Fig. 1*C*). *In utero* electroporation of this Mst3 shRNA at E14 resulted in migratory defects that were rescued by the reexpression of a shRNA-resistant Mst3-expressing construct. Although most (~50%) of the neurons expressing pSUPER vector or scrambled shRNA migrated into the cortical plate at E17, the majority (~60%) of Mst3-knockdown neurons remained stacked in the intermediate zone (Fig. 1*D*,*E*). To determine whether this migratory defect is associated with abnormal neuronal morphology, we examined leading process formation in knockdown neurons at the intermediate zone. Notably, whereas control neurons formed a single leading process pointing toward the pial surface, most Mst3-knockdown neurons in the intermediate zone exhibited disrupted neuronal polarity with no extended process (Fig. 1*F*,*G*).

Mst3 knockdown leads to altered neuronal positioning and cortical activity

The accumulation of Mst3-knockdown neurons in the intermediate zone may be due to either the inhibition or delay of neuronal migration. Intriguingly, whereas only some of the Mst3-knockdown neurons migrated up into the cortical plate at E18 (Fig. 1*H*,*I*), most of them ultimately migrated to the upper layers of the cortical plate at P2 and P5 (Fig. 2*A*,*B*). These results suggest that Mst3 knockdown delayed rather than arrested neuronal migration. However, although the neurons were able to migrate up into the cortical plate, the final positioning of Mst3-knockdown neurons was abnormal. Compared with the control neurons, the cell bodies of which were deposited in the upper part of layers II–IV (Cutl1+), the knockdown neurons were located in a relatively deeper part of layers II–IV. In addition to the positional defect, Mst3 knockdown also led to abnormal neuronal morphology and impaired dendrite development. The Mst3-knockdown neurons exhibited significantly shorter apical dendrites, altered orientation, and distorted cell bodies compared with the control neurons (Fig. 2*C*–*E*). Collectively, these findings suggest that Mst3 is important for the precise positioning and morphogenesis of neurons in the cerebral cortex.

To determine whether the migration defect and morphological abnormalities caused by Mst3 knockdown leads to altered cortical excitability, we performed whole-cell recordings of the pyramidal neurons in upper layers II–III. Intriguingly, the frequency of spontaneous EPSCs was significantly lower in the Mst3-knockdown pyramidal neurons compared with the control neurons (Fig. 2*F*–*H*). Therefore, Mst3 knockdown impaired the excitatory synaptic transmission of the pyramidal neurons in the upper cortical layers.

Mst3 kinase activity is important for neuronal migration

The prominent kinase activity of Mst3 from E14 to E17 prompted us to investigate whether Mst3-regulated radial migration is dependent on its kinase activity. To generate a kinase-dead Mst3 mutant (Mst3-KD), the ATP-binding site (Lys53) was substituted with arginine (Fig. 3*A*). Loss of kinase activity of Mst3-KD was confirmed by its inability to phosphorylate histone H1 in an *in vitro* phosphorylation assay (Fig. 3*A*). We subsequently generated shRNA-resistant forms of Mst3 WT and Mst3-KD (Fig. 3*B*). Notably, reexpression of Mst3-WT but not KD fully restored normal migration and neuronal morphology in Mst3-knockdown cortices (Fig. 3*C*–*F*). Nonetheless, overexpression of Mst3-KD alone does not affect the neuronal migration (Fig. 3*G*,*H*). Given the relatively high Mst3 activity in mouse brains at embryonic stages (E14–E17), the expression of Mst3-KD may be ineffective to compete with endogenous Mst3 and inhibit its activity and functions in migrating neurons. This suggests that Mst3 kinase activity is important for radial migration. Therefore, understanding the regulation of Mst3 kinase activity may provide insights into the molecular mechanisms of neuronal migration.

Prediction of potential phosphorylation sites by a computational method (Obenauer et al., 2003) identified various potential phosphorylation sites in Mst3 recognized by various kinases, including GSK3, Cdk5, JNK, MEK, and PKA. After treating cortical neurons with different kinase inhibitors, only the Cdk5 inhibitor dramatically reduced autophosphorylation (p-Mst3; Fig. 4*A*) and thus Mst3 activity. Furthermore, Mst3 kinase activity was reduced in *cdk5*-knock-out mouse brains (Fig. 4*B*). These results suggest that Cdk5 regulates Mst3 kinase activity. Indeed, we found that active Cdk5 phosphorylated Mst3 (Fig. 4*C*) and endogenous Mst3 phosphorylation were significantly attenuated in *cdk5*-knock-out brains (Fig. 4*D*). These findings suggest that Mst3 is phosphorylated by Cdk5 *in vivo*. Three sites on Mst3, Ser4, Ser79, and Ser369, were identified as potential Cdk5 phosphorylation sites (Fig. 4*E*). We subsequently generated phosphorylation-deficient mutants by mutating the Ser4, Ser79, or Ser369 site to alanine. Mutation of Ser79, but not the other two sites, abolished Cdk5-dependent Mst3 phosphorylation (Fig. 4*F*), indicating that Ser79 is the major Cdk5 phosphorylation site. To further confirm this result, we raised a phosphospecific Mst3 antibody against phosphorylated Mst3 at Ser79 (p-S79 Mst3). The p-S79 Mst3 antibody specifically recognized phosphorylated Mst3 protein after Cdk5 phosphorylation (Fig. 4*G*,*H*). Consistently, the Ser79 phosphorylation of Mst3 was dramatically reduced in *cdk5*-knock-out mouse brains (Fig. 4*I*), corroborating Mst3 as an *in vivo* substrate of Cdk5.

To investigate whether Cdk5-dependent Mst3 phosphorylation is important for radial migration, we reexpressed Mst3 WT and S79A mutant in Mst3-knockdown cortices. Mst3 WT fully restored normal migration, whereas reexpression of the Mst3 S79A mutant failed to rescue the migration defects and altered the neuronal morphology of Mst3-knockdown neurons (Fig. 4*J*–*L*). Similar to Mst3 KD, the S79A mutant alone has no effect on neuronal migration (Figs. 3*G*,*H*, 4*M*,*N*). Therefore, Cdk5-dependent phosphorylation of Mst3 at Ser79 is important for Mst3 kinase activity and thus proper neuronal migration.

←

(*Figure legend continued.*) percentages of neurons with unipolar/bipolar, no, and multiple processes. $^{**}p < 0.01$ versus pSUPER, $n = 3$, Student's *t* test, mean ± SEM. More than 200 GFP$^+$ neurons from six brains were analyzed in each group. ***H***, Representative images of E18 cortical sections stained with GFP antibody (green) and TO-PRO-3 (blue). ***I***, Quantification of the distribution of GFP$^+$ neurons in ***H***. $^{*}p < 0.05$, $n = 3$, Student's *t* test, mean ± SEM. More than 300 GFP$^+$ neurons from four brains were analyzed in each group.

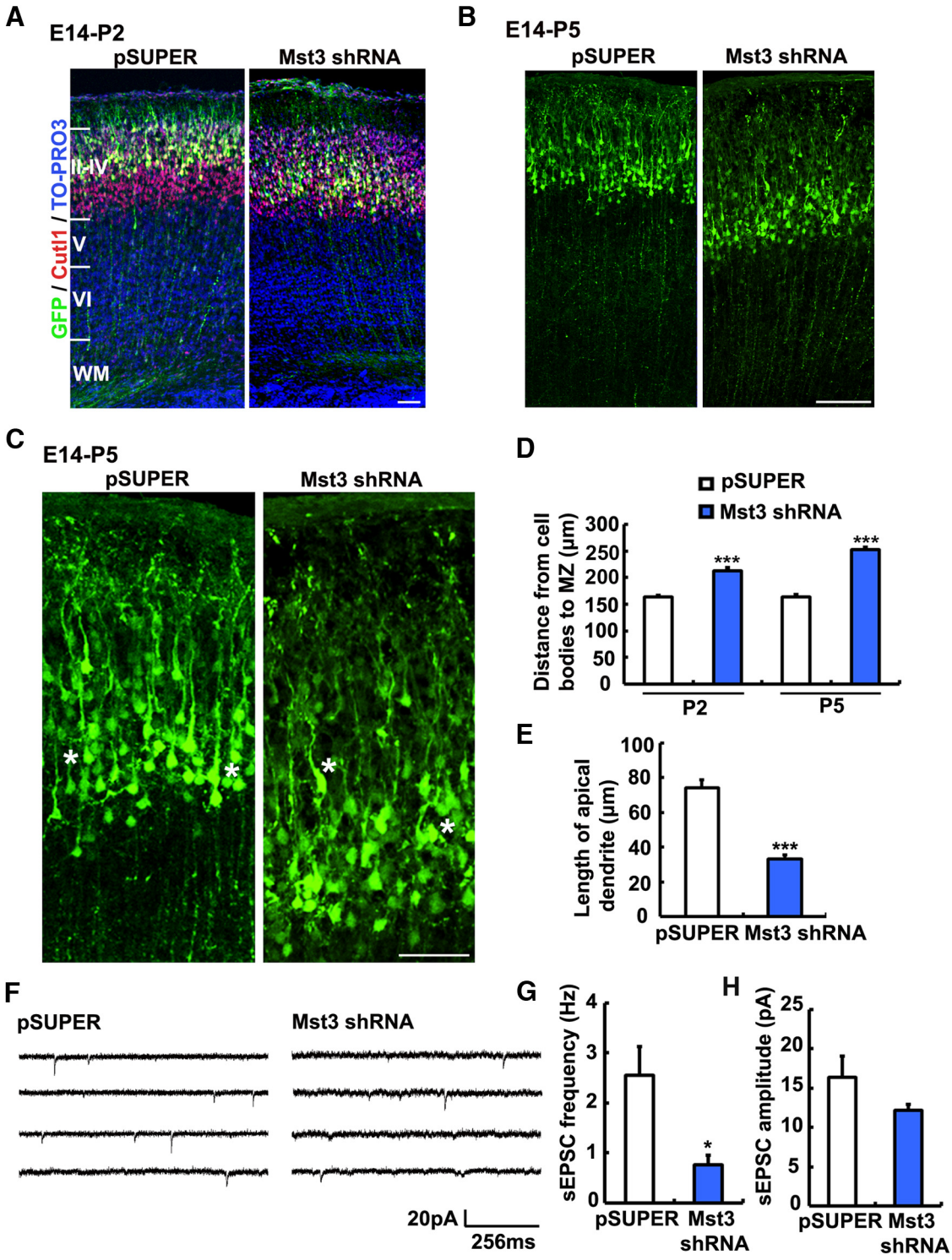

Figure 2. Mst3 knockdown perturbs neuronal positioning and dendritogenesis. ***A***, ***B***, Mst3 knockdown perturbed the final positions of layer II–IV neurons. E14 mouse embryos were electroporated with GFP expression construct and pSUPER or Mst3 shRNA by *in utero* electroporation. Mouse brains were collected at P2 (***A***) or P5 (***B***) and stained for GFP (green), Cutl1 (layer II–IV marker, red), and TO-PRO-3 (nuclear marker, blue) (***A***) or GFP alone (***B***). Scale bar, 100 μm. ***C***, Mst3 knockdown altered neuronal morphology and reduced apical dendrite length. E14 mouse embryos were electroporated with GFP expression construct and pSUPER or Mst3 shRNA by *in utero* electroporation. Brains were collected at P5 and stained for GFP alone. Asterisks indicate representative neurons. Scale bar, 50 μm. ***D***, Quantification of the distance from GFP $^+$ neuron cell bodies to the pial surface in ***A*** and ***B***. $^{***}p < 0.001$, $n = 3$, Student's *t* test, mean ± SEM. More than 200 GFP $^+$ neurons from three brains were analyzed in each group. ***E***, Quantification of the length of apical dendrites of GFP $^+$ neurons in ***C***. $^{***}p < 0.001$, $n = 3$, Student's *t* test, mean ± SEM. More than 200 GFP $^+$ neurons from three brains were analyzed in each group. ***F–H***, Spontaneous glutamatergic synaptic activity [i.e., spontaneous EPSCs (sEPSCs)] was altered in Mst3-knockdown neurons. ***F***, Representative traces of sEPSCs were recorded in layer II–III pyramidal neurons of pSUPER- and Mst3 shRNA-electroporated cortices from P15–P20. Mean frequencies (***G***) and mean amplitudes (***H***) of sEPSCs in layer II–III pyramidal neurons of pSUPER- and Mst3 shRNA-electroporated sections. $^*p < 0.05$, $n = 3$, Student's *t* test, mean ± SEM. Six to eight neurons from three mice were analyzed in each group.

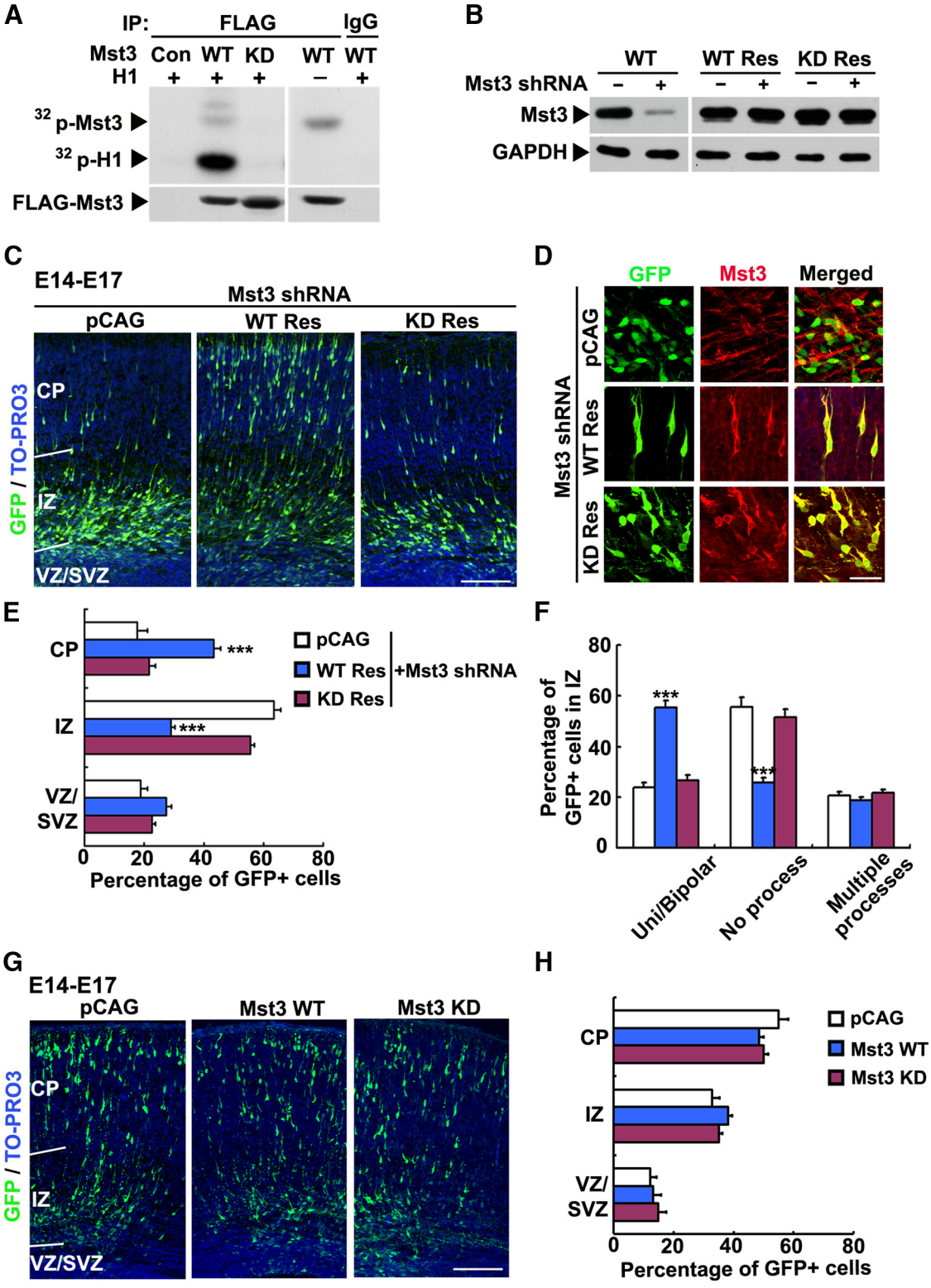

Figure 3. Mst3 activity is required for proper radial migration. ***A***, The KD mutant (Lys53 ⟶ Arg, K53R) of Mst3 lacked kinase activity. *In vitro* kinase assay using histone H1 as a substrate. ***B***, Overexpression of RNAi-resistant Mst3 (WT Res or KD Res) restored Mst3 protein expression in HEK293T cells expressing Mst3 shRNA. ***C–F***, Kinase activity of Mst3 is important for radial migration. ***C***, Expression of Mst3 WT Res, but not the Mst3 KD Res, rescued the delayed migration of cortical neurons upon Mst3 knockdown. Scale bar, 100 μm. ***D***, Images of neurons in the upper intermediate zone (IZ) stained with GFP antibody (green) and Mst3 antibody (red). Scale bar, 25 μm. ***E***, Quantification of the distribution of GFP$^+$ neurons in the brain sections electroporated with Mst3 shRNA together with Mst3 WT Res or KD Res. ***$p < 0.001$, $n = 3$, Student's t test, mean ± SEM. ***F***, Quantification of the percentages of neurons with unipolar/bipolar, no, or multiple processes. ***$p < 0.001$, $n = 3$, Student's t test, mean ± SEM. More than 200 GFP$^+$ neurons from six brains were analyzed in each group. ***G***, Expression of Mst3 WT or Mst3 KD had no effect on neuronal migration. Scale bar, 100 μm. ***H***, Quantification of the distribution of GFP$^+$ neurons in the brain sections electroporated with pCAG, Mst3 WT, or Mst3 KD. $n = 3$, Student's t test, mean ± SEM.

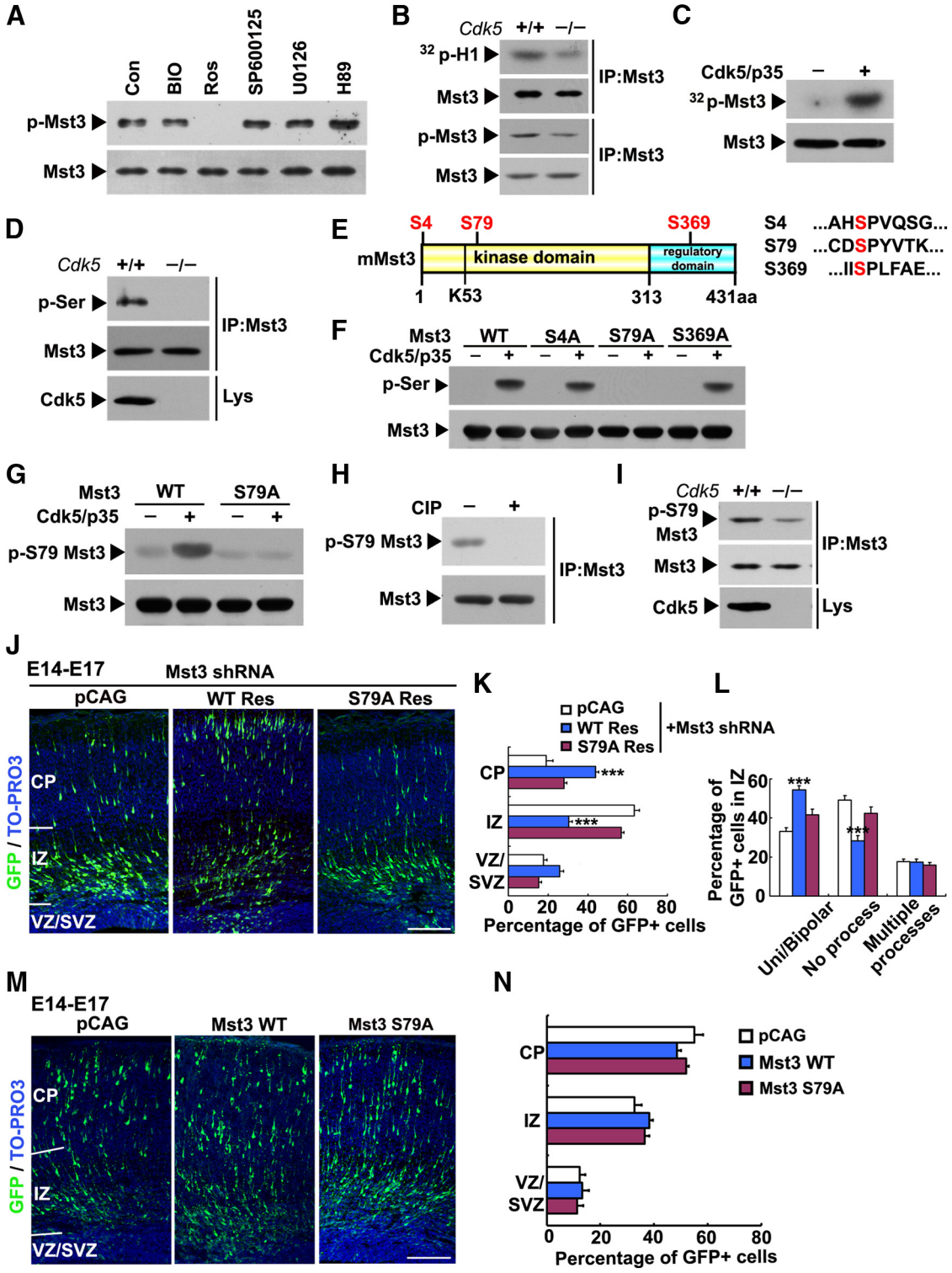

Figure 4. Cdk5-dependent phosphorylation of Mst3 at Ser79 is important for radial migration. ***A***, Cdk5 inhibition abolishes Mst3 activation. Cultured cortical neurons were treated for 1 h with different specific kinase inhibitors: 200 nM BIO (GSK3), 10 μM Ros (Cdk5), 10 μM SP600125 (JNK), 100 nM U0126 (MEK), or 20 μM H89 (PKA). Mst3 kinase activity was examined by Western blot analysis for Mst3 autophosphorylation at Thr178 (p-Mst3). ***B***, Mst3 kinase activity was reduced in Cdk5 $^{-/-}$ mouse brains. The brain lysates of E18 Cdk5 $^{-/-}$ mice were immunoprecipitated with anti-Mst3 antibody and subjected to a kinase assay ($n = 3$; p-H1: 0.53 $\pm$ 0.05-fold in Cdk5 $^{-/-}$ brains, mean $\pm$ SEM, $p < 0.001$, Student's t test) or Western blot analysis with p-Mst3 antibody ($n = 4$; p-Mst3: 0.49 $\pm$ 0.07-fold in Cdk5 $^{-/-}$ brains, mean $\pm$ SEM, $p < 0.001$, Student's t test). ***C***, Direct phosphorylation of Mst3 by Cdk5 in an *in vitro* phosphorylation assay. ***D***, Serine phosphorylation of Mst3 was dramatically reduced in Cdk5 $^{-/-}$ brains blotted with p-(Ser) CDK substrate antibody. ***E***, Schematic diagram indicating the domains of Mst3 and mutation sites described in the text. ***F***, Cdk5 phosphorylated Mst3 at Ser79. Western blot analysis was performed using anti-phospho-serine (p-Ser CDK substrate) antibody. ***G***, Generation of a phosphospecific antibody against Mst3 at Ser79 (p-S79 Mst3). Mst3 protein was overexpressed in HEK293T cells, immunoprecipitated by anti-Mst3 antibody, and incubated with Cdk5/p35 complex for the *in vitro* phosphorylation assay. Phosphorylated Mst3 was detected by a phosphospecific antibody targeting the Ser79 site of Mst3. ***H***, Calf intestinal phosphatase (CIP) treatment abolished Ser79 phosphorylation of Mst3. ***I***, Mst3 phosphorylation at Ser79 was attenuated in Cdk5 $^{-/-}$ mouse brains. ($n = 5$; p-S79 Mst3: 0.58 $\pm$ 0.01-fold in Cdk5 $^{-/-}$ brains, mean $\pm$ SEM, $p < 0.001$; Student's t test). ***J–L***, The Ser79 phosphodeficient mutant of Mst3 (S79A) failed to rescue the delayed migration of cortical neurons upon Mst3 knockdown. (*Figure legend continues.*)

Mst3 regulates actin dynamics and RhoA activity

Next, we investigated how Mst3 and its kinase activity regulate neuronal migration. Mst3 was enriched in growing neurite tips of neurons, where it colocalized with F-actin staining (Fig. 5*A*). Notably, Mst3 knockdown in neurons substantially increased the ratio of F-actin to G-actin (Fig. 5*B*,*C*), suggesting that Mst3 regulates the polymerization status of the actin cytoskeleton. To determine how Mst3 regulates the morphology of migrating neurons, Mst3 shRNA was introduced into cortical neurons cultured from E14 embryos and growth cone morphology was examined 1 d later. Mst3 knockdown resulted in remarkably increased growth cone collapse. Interestingly, such defects were largely rescued by Y27632 (RI), a pharmacological inhibitor of RhoA signaling (Fig. 5*D*,*E*). Together with the interaction between Mst3 and RhoA, but not the other two important Rho-GTPases (i.e., Rac1 and Cdc42, data not shown; Fig. 5*F*), these results suggest that RhoA is a downstream signaling molecule of Mst3. Importantly, Mst3 knockdown led to RhoA activation, whereas Mst3 overexpression inhibited RhoA activity in cultured neurons (Fig. 5*G*,*H*). These findings suggest that Mst3 plays important roles in the regulation of actin dynamics and RhoA inhibition.

Negative regulation of RhoA by Mst3 phosphorylation is important for radial migration

Mst3 phosphorylated RhoA at serine residue(s) (Fig. 6*A*). Mass spectrometry and 3D structural analysis identified two potential Mst3 phosphorylation sites on RhoA: Ser26 and Ser160 (Ihara et al., 1998). An *in vitro* phosphorylation assay confirmed that Mst3 phosphorylates RhoA at Ser26 (Fig. 6*B*). Importantly, blocking the Mst3-dependent phosphorylation of RhoA at Ser26 enhanced its GTPase activity (Fig. 6*C*), suggesting that Ser26 phosphorylation at RhoA negatively regulates its activity. To determine whether Mst3-dependent RhoA phosphorylation is important for neuronal migration, we overexpressed RhoA WT or S26A in E14 mouse brains. Overexpression of RhoA WT significantly inhibited neuronal migration and disrupt normal neuronal polarization, whereas overexpression of RhoA S26A, which has higher RhoA activity, led to a more severe defect in neuronal migration and polarization (Fig. 6*D*,*E*). Similar to the effect observed in Mst3-knockdown cortices, RhoA WT or S26A-expressing migrating neurons exhibited an abnormal morphology with no neuronal polarity or processes (Fig. 6*F*). Moreover, inhibition of RhoA activity by suppressing the RhoA protein expression restored migration and neuronal morphology defects in Mst3-knockdown neurons (Fig. 6*G–I*). Together, these findings reveal a critical role of Mst3 in the regulation of radial migration via the inhibition of RhoA activity.

Discussion

In this study, we report that Mst3 is a critical regulator of corticogenesis through controlling the final positioning and morphogenesis of migrating neurons. Our results show that the activity of Mst3 is regulated by Cdk5 phosphorylation and activated Mst3 in turn inhibits RhoA activity, thus modulating the actin cytoskeleton of migrating neurons. Together with previous reports on the regulation of RhoA-dependent actin dynamics by Cdk5 (Ye et al., 2012), these findings suggest that Cdk5 regulates neuronal migration through integration of various kinase signaling pathways, including that mediated by Mst3.

It has become increasingly clear that subtle alterations in neuronal morphogenesis may underlie the pathophysiology of various neurological disorders. For example, aberrant dendritic patterning and altered spine morphology have been implicated in psychiatric disorders with delayed onset, such as autism spectrum disorders (de Anda et al., 2012). Therefore, it is important to understand how pyramidal neurons acquire their dendritic morphology after terminal translocation. Here, we show that Mst3 knockdown retards the migration of cortical neurons, resulting in mispositioning of Mst3-deficient neurons. Importantly, the Mst3-depleted neurons exhibit aberrant dendrite morphology. These findings collectively suggest that Mst3 plays multiple roles in different cellular events during corticogenesis, including neuronal migration and dendrite development, in a cell-autonomous manner. In support of this notion, we found that dendrite extension and arborization was inhibited in cultured neurons after Mst3 knockdown (data not shown). However, given that Mst3 kinase activity is robust in embryonic brains and becomes much lower in postnatal brains, it is likely that the defect in synaptic transmission in Mst3-depleted cortex is due to the mispositioning of neurons rather than being the direct result of Mst3 knockdown. Further studies on how Mst3 knockdown may affect circuit connection among layer II–IV pyramidal neurons may provide insights on the pathogenesis of psychiatric disorders.

Inhibition of RhoA activity is required for F-actin depolymerization at the tip of leading process during multipolar-to-bipolar transition (Pacary et al., 2011). Nonetheless, how RhoA activity is regulated in migrating neurons remains largely unknown. We found that silencing Mst3 in cultured neurons results in enhanced RhoA activity and increased F-actin content, whereas depletion of the RhoA protein expression rescues the radial migration defect of the Mst3-knockdown neurons. These results support the hypothesis that the inactivation of RhoA activity by Mst3 causes F-actin depolymerization, ultimately allowing the polarization of neurons and their exit from the intermediate zone, which is an initial critical step in radial migration. In addition to Mst3, RhoA activity is regulated through phosphorylation by other kinases, such as cAMP- and cGMP-dependent kinases (i.e., PKA and PKG; Ellerbroek et al., 2003). In addition, RhoA-dependent actin reorganization is modulated by various signaling regulators, including an atypical Rho-GTPase Rnd3 and p27 (Nguyen et al., 2006; Pacary et al., 2011). Interestingly, the activity and functions of these RhoA regulators can be modulated by phosphorylation. In particular, p27 and Mst3 are substrates of Cdk5 (Kawauchi et al., 2006, and present results). Cdk5-mediated phosphorylation of p27 or Mst3 leads to the inactivation of RhoA, suggesting that Cdk5 acts as a functional switch through phosphorylation of multiple substrates during the initiation of radial migration.

How does Mst3 regulate RhoA? The activity of RhoA is tightly regulated by three classes of regulatory proteins: guanine dissociation inhibitors, guanine nucleotide exchange factors (GEFs), and GTPase-activating proteins (Takai et al., 2001). In addition, the phosphorylation of Ser188 in the C-terminal region regulates RhoA activity by protecting the protein from ubiquitin/proteasome-

←

(*Figure legend continued.*) ***J***, Representative images at E17 were stained with anti-GFP antibody (green) and TO-PRO-3 (blue). Scale bar, 100 μm. ***K***, Quantification of the distribution of GFP$^+$ neurons. ***$p < 0.001$ versus pCAG+Mst3 shRNA; $n = 3$, Student's *t* test, mean ± SEM. ***L***, Quantification of the percentages of neurons with unipolar/bipolar, no, and multiple processes. More than 200 GFP$^+$ neurons from five brains were analyzed in each group. ***$p < 0.001$, $n = 3$, Student's *t* test, mean ± SEM. ***M***, The expression of Mst3 WT or Mst3 S79A had no effect on neuronal migration. Scale bar, 100 μm. ***N***, Quantification of the distribution of GFP$^+$ neurons in the brain sections electroporated with pCAG, Mst3 WT, or Mst3 S79A. $n = 3$, Student's *t* test, mean ± SEM.

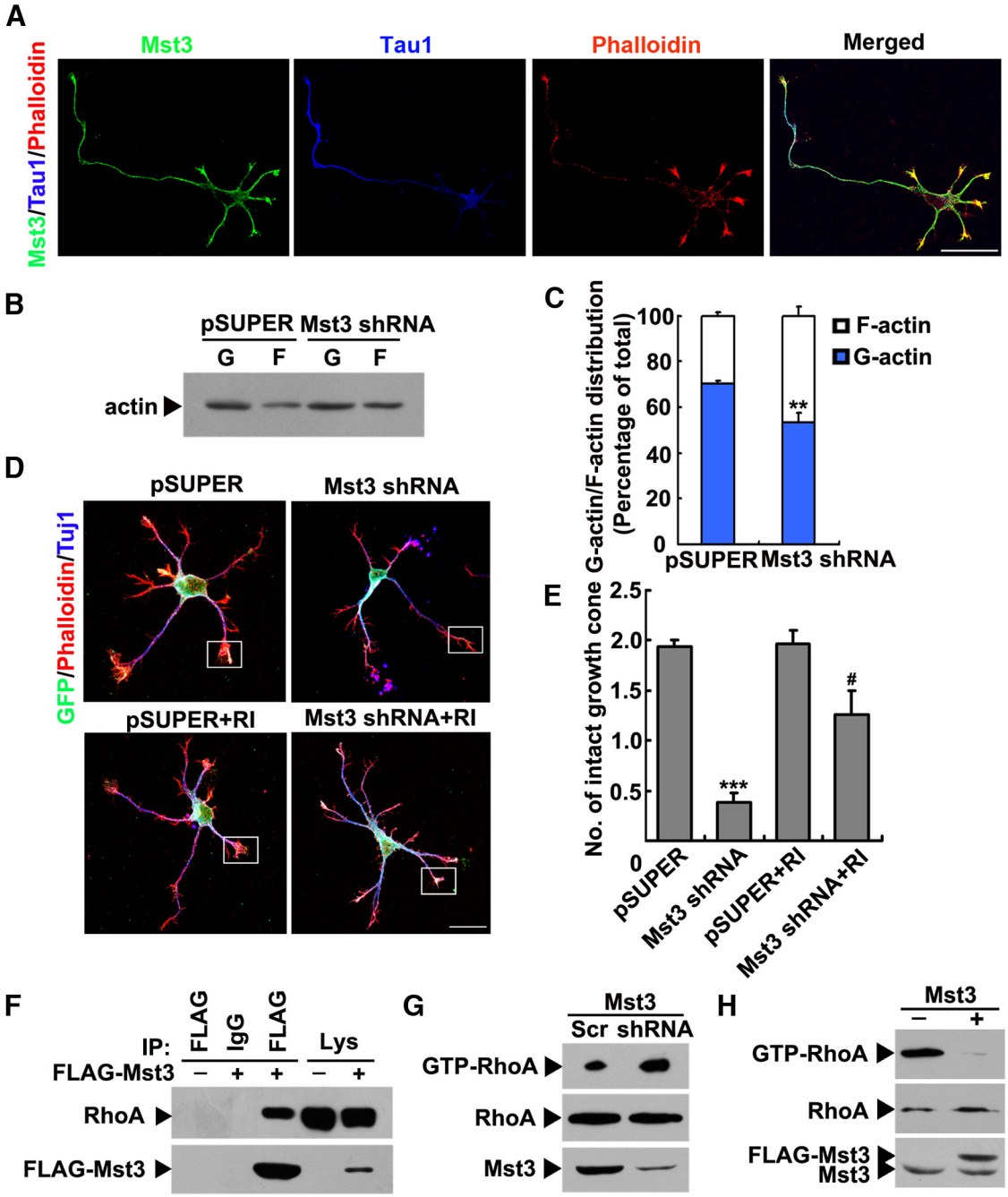

Figure 5. Mst3 regulates actin dynamics and RhoA activity. ***A***, Mst3 was concentrated in the F-actin-rich region. Cultured cortical neurons at 3 DIV were stained with anti-Mst3 (green) and anti-Tau1 (axon marker, blue) antibodies and fluorescently labeled phalloidin (F-actin marker, red). ***B***, ***C***, The G/F-actin ratio was lower in Mst3-knockdown cortical neurons. Cortical neurons were transfected with pSUPER or Mst3 shRNA. The F-actin and G-actin fractions were separated by SDS-PAGE and actin was quantified by Western blotting using anti-actin antibody. The F-actin (F; pellet fraction) and G-actin (G; supernatant fraction) pools are shown. ***C***, Quantification of G/F-actin ratio in the Mst3-knockdown cortical neurons in ***B***. $n = 4$, G/F-actin ratio, ~50% reduction, $^{**}p < 0.01$; Student's *t* test, mean ± SEM. ***D***, ***E***, Mst3 knockdown reduced the number of intact growth cones. Cortical neurons, transfected with GFP (green) and pSUPER or Mst3 shRNA, were treated with RI (Y27632). The fixed neurons were stained with anti-GFP (green) and anti-Tuj1 (βIII-tubulin marker, blue) antibodies and phalloidin (F-actin marker, red). ***E***, Quantification of the number of intact growth cones in ***D***. $^{***}p < 0.001$ versus pSUPER in the control condition; $\#p < 0.05$ versus pSUPER in the RI condition. $n = 3$, Student's *t* test, mean ± SEM. More than 300 GFP$^+$ neurons from three different experiments were analyzed in each group. ***F***, RhoA interacted with Mst3 in HEK293T cells. HEK293T cells expressing FLAG-Mst3 and RhoA were lysed and immunoprecipitated with anti-FLAG antibody. Mouse IgG was used as a negative control. ***G***, RhoA activity was elevated in Mst3-knockdown cortical neurons. $n = 3$; GTP-RhoA: 2.02 ± 0.10-fold in Mst3 shRNA, mean ± SEM, $p < 0.001$, Student's *t* test. ***H***, Ectopic Mst3 expression reduced RhoA activity in cortical neurons. $n = 3$, GTP-RhoA: 0.19 ± 0.09-fold in Mst3 overexpressing condition, mean ± SEM, $p < 0.001$, Student's *t* test.

mediated degradation (Rolli-Derkinderen et al., 2005). Our results show that the phosphorylation of RhoA at Ser26 by Mst3 negatively regulates its RhoA GTPase activity. Interestingly, Ser26 is adjacent to Lys27, which is a residue in the Switch I region of RhoA that is critical for the specific interactions between RhoA and its GEFs (Ihara et al., 1998). Therefore, it would be interesting to determine whether this specific phosphorylation of RhoA alters its association with GEFs during neuronal migration. Furthermore, given that Ser26 is conserved among different Rho members, phosphorylation at this specific site may serve as a

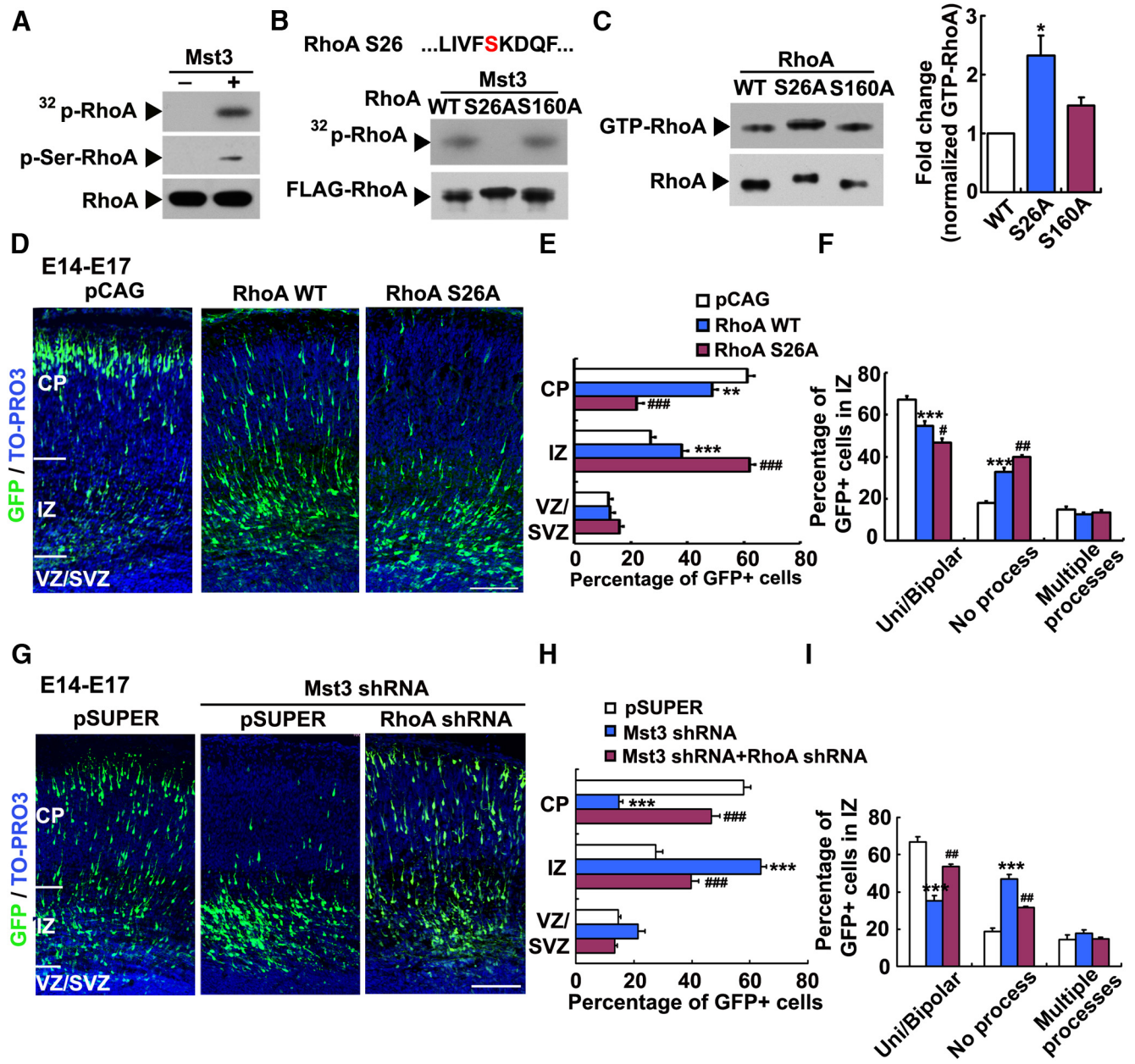

Figure 6. Mst3 regulates neuronal migration via the modulation of RhoA activity. ***A***, Mst3 phosphorylated RhoA at serine residue(s). *In vitro* phosphorylation assay (top) and Western blotting for p-Ser antibody (middle), and total RhoA (bottom). ***B***, Mst3 phosphorylated RhoA at Ser26. The Mst3 phosphorylation site on Ser26 site is shown. WT and two phosphodeficient mutants of RhoA at putative Mst3 phosphorylation sites (S26A and S160A) were subjected to an *in vitro* phosphorylation assay. ***C***, Blockade of RhoA phosphorylation at Ser26 increased the GTPase activity of RhoA. HEK293T cells expressing WT, S26A, or S160A mutants of RhoA were pulled down by anti-FLAG antibody and subjected to GTPase activity assay. Fold change of GTP-RhoA (mean ± SEM, $^{*}p < 0.01$, $n = 3$, Student's *t* test). ***D***, Mst3-dependent RhoA phosphorylation is important for radial migration. E14 mouse brains were electroporated with pCAG vector, RhoA WT, or RhoA S26A. Representative mouse brain sections were stained with anti-GFP antibody (green) and TO-PRO-3 (blue). Scale bar, 100 μm. ***E***, Quantification of the distribution of GFP $^{+}$ neurons. $^{***}p < 0.001$, $^{**}p < 0.01$ versus pCAG; $^{###}p < 0.001$ versus RhoA WT; $n = 3$, Student's *t* test, mean ± SEM. ***F***, Quantification of the percentages of neurons with unipolar/bipolar, no, and multiple processes. $^{***}p < 0.001$ versus pCAG; $^{\#}p < 0.05$, $^{\#\#}p < 0.01$ versus RhoA WT, $n = 3$, Student's *t* test, mean ± SEM. More than 300 GFP $^{+}$ neurons from five brains were analyzed in each group. ***G***, RhoA knockdown rescued the Mst3-dependent delayed migration. E14 mouse brains were electroporated with GFP construct together with pSUPER, Mst3 shRNA, or Mst3 shRNA together with RhoA shRNA. Representative sections of E17 brains were stained with anti-GFP antibody (green) and TO-PRO-3 (blue). Scale bar, 100 μm. ***H***, Quantification of the distribution of GFP $^{+}$ neurons. $^{***}p < 0.001$ versus pSUPER; $^{###}p < 0.001$ versus Mst3 shRNA, $n = 3$, Student's *t* test, mean ± SEM. ***I***, Quantification of the percentages of neurons with unipolar/bipolar, no, and multiple processes. $^{***}p < 0.001$ versus pSUPER; $^{\#\#}p < 0.01$ versus Mst3 shRNA, $n = 3$, Student's *t* test, mean ± SEM. More than 300 GFP $^{+}$ neurons from six brains were analyzed in each group.

general negative regulatory mechanism for members of this small GTPase family (Madaule and Axel, 1985; Chardin et al., 1988; Fagan et al., 1994).

Although phosphorylation of Mst3 at Ser79 results in the increase of its kinase activity, its underlying molecular mechanism remains to be elucidated. Our preliminary results show that suppression of Ser79 phosphorylation apparently does not affect the substrate-binding or ATP-binding abilities of Mst3 (data not shown). Structural analysis reveals that Ser79 is located near the C-helix within the kinase domain, which is an element important for the conformational change of the kinase domain during catalysis (Ko et al., 2010). Therefore, Ser79 phosphorylation of Mst3 may be important for the catalytic activity of the kinase. Although Ser79 is conserved among different members of the

Mst family (Record et al., 2010), it would be intriguing to determine whether this serine phosphorylation regulates the kinase activities of other Mst members and thus their functions during neurodevelopment. It will also be important to determine whether the status of Ser79 phosphorylation of Mst3 is altered in animal models of neuropsychiatric disorders. Further characterization of this serine phosphorylation will provide important insights into the pathogenesis of neurodevelopmental disorders such as autism spectrum disorders.

In conclusion, our results demonstrate that the Cdk5–Mst3 pathway controls the precise organization of the actin cytoskeleton during initiation of neuronal migration. The convergence of various kinase signaling pathways toward cytoskeletal organization and remodeling during neuronal migration indicates that the patterning and lamination of the cerebral cortex is under precise regulation by a complex and coordinated system of biochemical signaling mechanisms.

References

Ayala R, Shu T, Tsai LH (2007) Trekking across the brain: the journey of neuronal migration. Cell 128:29–43. CrossRef Medline

Bielas S, Higginbotham H, Koizumi H, Tanaka T, Gleeson JG (2004) Cortical neuronal migration mutants suggest separate but intersecting pathways. Annu Rev Cell Dev Biol 20:593–618. CrossRef Medline

Chardin P, Madaule P, Tavitian A (1988) Coding sequence of human rho cDNAs clone 6 and clone 9. Nucl Acids Res 16:2717. CrossRef Medline

Conery AR, Sever S, Harlow E (2010) Nucleoside diphosphate kinase Nm23–H1 regulates chromosomal stability by activating the GTPase dynamin during cytokinesis. Proc Natl Acad Sci U S A 107:15461–15466. CrossRef Medline

Creppe C, Malinouskaya L, Volvert ML, Gillard M, Close P, Malaise O, Laguesse S, Cornez I, Rahmouni S, Ormenese S, Belachew S, Malgrange B, Chapelle JP, Siebenlist U, Moonen G, Chariot A, Nguyen L (2009) Elongator controls the migration and differentiation of cortical neurons through acetylation of alpha-tubulin. Cell 136:551–564. CrossRef Medline

de Anda FC, Rosario AL, Durak O, Tran T, Gräff J, Meletis K, Rei D, Soda T, Madabhushi R, Ginty DD, Kolodkin AL, Tsai LH (2012) Autism spectrum disorder susceptibility gene TAOK2 affects basal dendrite formation in the neocortex. Nat Neurosci 15:1022–1031. CrossRef Medline

Deutsch SI, Burket JA, Katz E (2010) Does subtle disturbance of neuronal migration contribute to schizophrenia and other neurodevelopmental disorders? Potential genetic mechanisms with possible treatment implications. Eur Neuropsychopharmacol 20:281–287. CrossRef Medline

Douglas RJ, Martin KA (2004) Neuronal circuits of the neocortex. Annu Rev Neurosci 27:419–451. CrossRef Medline

Ellerbroek SM, Wennerberg K, Burridge K (2003) Serine phosphorylation negatively regulates RhoA in vivo. J Biol Chem 278:19023–19031. CrossRef Medline

Emoto K, Parrish JZ, Jan LY, Jan YN (2006) The tumour suppressor Hippo acts with the NDR kinases in dendritic tiling and maintenance. Nature 443:210–213. CrossRef Medline

Fagan KP, Oliveira L, Pittler SJ (1994) Sequence of rho small GTP-binding protein cDNAs from human retina and identification of novel 5′ end cloning artifacts. Exp Eye Res 59:235–237. CrossRef Medline

Fang WQ, Ip JP, Li R, Ng YP, Lin SC, Chen Y, Fu AK, Ip NY (2011) Cdk5-mediated phosphorylation of Axin directs axon formation during cerebral cortex development. J Neurosci 31:13613–13624. CrossRef Medline

Fu WY, Chen Y, Sahin M, Zhao XS, Shi L, Bikoff JB, Lai KO, Yung WH, Fu AK, Greenberg ME, Ip NY (2007) Cdk5 regulates EphA4-mediated dendritic spine retraction through an ephexin1-dependent mechanism. Nat Neurosci 10:67–76. CrossRef Medline

Gleeson JG, Walsh CA (2000) Neuronal migration disorders: from genetic diseases to developmental mechanisms. Trends Neurosci 23:352–359. CrossRef Medline

Guerrier S, Coutinho-Budd J, Sassa T, Gresset A, Jordan NV, Chen K, Jin WL, Frost A, Polleux F (2009) The F-BAR domain of srGAP2 induces membrane protrusions required for neuronal migration and morphogenesis. Cell 138:990–1004. CrossRef Medline

Guerrini R, Dobyns WB, Barkovich AJ (2008) Abnormal development of the human cerebral cortex: genetics, functional consequences and treatment options. Trends Neurosci 31:154–162. CrossRef Medline

Hall A (1994) Small GTP-binding proteins and the regulation of the actin cytoskeleton. Annu Rev Cell Biol 10:31–54. CrossRef Medline

Ihara K, Muraguchi S, Kato M, Shimizu T, Shirakawa M, Kuroda S, Kaibuchi K, Hakoshima T (1998) Crystal structure of human RhoA in a dominantly active form complexed with a GTP analogue. J Biol Chem 273:9656–9666. CrossRef Medline

Ip JP, Shi L, Chen Y, Itoh Y, Fu WY, Betz A, Yung WH, Gotoh Y, Fu AK, Ip NY (2012) alpha2-chimaerin controls neuronal migration and functioning of the cerebral cortex through CRMP-2. Nat Neurosci 15:39–47. CrossRef Medline

Irwin N, Li YM, O'Toole JE, Benowitz LI (2006) Mst3b, a purine-sensitive Ste20-like protein kinase, regulates axon outgrowth. Proc Natl Acad Sci U S A 103:18320–18325. CrossRef Medline

Kawauchi T, Hoshino M (2008) Molecular pathways regulating cytoskeletal organization and morphological changes in migrating neurons. Dev Neurosci 30:36–46. CrossRef Medline

Kawauchi T, Chihama K, Nabeshima Y, Hoshino M (2006) Cdk5 phosphorylates and stabilizes p27kip1 contributing to actin organization and cortical neuronal migration. Nat Cell Biol 8:17–26. CrossRef Medline

Ko TP, Jeng WY, Liu CI, Lai MD, Wu CL, Chang WJ, Shr HL, Lu TJ, Wang AH (2010) Structures of human MST3 kinase in complex with adenine, ADP and Mn2+. Acta Crystallogr D Biol Crystallogr 66:145–154. CrossRef Medline

Lehtinen MK, Yuan Z, Boag PR, Yang Y, Villén J, Becker EB, DiBacco S, de la Iglesia N, Gygi S, Blackwell TK, Bonni A (2006) A conserved MST-FOXO signaling pathway mediates oxidative-stress responses and extends life span. Cell 125:987–1001. CrossRef Medline

Ling P, Lu TJ, Yuan CJ, Lai MD (2008) Biosignaling of mammalian Ste20-related kinases. Cell Signal 20:1237–1247. CrossRef Medline

Lorber B, Howe ML, Benowitz LI, Irwin N (2009) Mst3b, an Ste20-like kinase, regulates axon regeneration in mature CNS and PNS pathways. Nat Neurosci 12:1407–1414. CrossRef Medline

LoTurco JJ, Bai J (2006) The multipolar stage and disruptions in neuronal migration. Trends Neurosci 29:407–413. CrossRef Medline

Madaule P, Axel R (1985) A novel ras-related gene family. Cell 41:31–40. CrossRef Medline

Meller R, Thompson SJ, Lusardi TA, Ordonez AN, Ashley MD, Jessick V, Wang W, Torrey DJ, Henshall DC, Gafken PR, Saugstad JA, Xiong ZG, Simon RP (2008) Ubiquitin proteasome-mediated synaptic reorganization: a novel mechanism underlying rapid ischemic tolerance. J Neurosci 28:50–59. CrossRef Medline

Nadarajah B, Parnavelas JG (2002) Modes of neuronal migration in the developing cerebral cortex. Nat Rev Neurosci 3:423–432. CrossRef Medline

Nguyen L, Besson A, Heng JI, Schuurmans C, Teboul L, Parras C, Philpott A, Roberts JM, Guillemot F (2006) p27kip1 independently promotes neuronal differentiation and migration in the cerebral cortex. Genes Dev 20:1511–1524. CrossRef Medline

Obenauer JC, Cantley LC, Yaffe MB (2003) Scansite 2.0: Proteome-wide prediction of cell signaling interactions using short sequence motifs. Nucleic Acids Res 31:3635–3641. CrossRef Medline

Pacary E, Heng J, Azzarelli R, Riou P, Castro D, Lebel-Potter M, Parras C, Bell DM, Ridley AJ, Parsons M, Guillemot F (2011) Proneural transcription factors regulate different steps of cortical neuron migration through Rnd-mediated inhibition of RhoA signaling. Neuron 69:1069–1084. CrossRef Medline

Rashid T, Banerjee M, Nikolic M (2001) Phosphorylation of Pak1 by the p35/Cdk5 kinase affects neuronal morphology. J Biol Chem 276:49043–49052. CrossRef Medline

Record CJ, Chaikuad A, Rellos P, Das S, Pike AC, Fedorov O, Marsden BD, Knapp S, Lee WH (2010) Structural comparison of human mammalian ste20-like kinases. PLoS One 5:e11905. CrossRef Medline

Rolli-Derkinderen M, Sauzeau V, Boyer L, Lemichez E, Baron C, Henrion D, Loirand G, Pacaud P (2005) Phosphorylation of serine 188 protects RhoA from ubiquitin/proteasome-mediated degradation in vascular smooth muscle cells. Circ Res 96:1152–1160. CrossRef Medline

Shi L, Fu WY, Hung KW, Porchetta C, Hall C, Fu AK, Ip NY (2007) Alpha2-chimaerin interacts with EphA4 and regulates EphA4-dependent growth cone collapse. Proc Natl Acad Sci U S A 104:16347–16352. CrossRef Medline

Sidman RL, Rakic P (1973) Neuronal migration, with special reference to developing human brain: a review. Brain Res 62:1–35. CrossRef Medline

Singh KK, Ge X, Mao Y, Drane L, Meletis K, Samuels BA, Tsai LH (2010) Dixdc1 is a critical regulator of DISC1 and embryonic cortical development. Neuron 67:33–48. CrossRef Medline

Su SC, Tsai LH (2011) Cyclin-dependent kinases in brain development and disease. Annu Rev Cell Dev Biol 27:465–491. CrossRef Medline

Takai Y, Sasaki T, Matozaki T (2001) Small GTP-binding proteins. Physiol Rev 81:153–208. Medline

Tanaka T, Serneo FF, Tseng HC, Kulkarni AB, Tsai LH, Gleeson JG (2004) Cdk5 phosphorylation of doublecortin ser297 regulates its effect on neuronal migration. Neuron 41:215–227. CrossRef Medline

Valiente M, Marin O (2010) Neuronal migration mechanisms in development and disease. Curr Opin Neurobiol

Wegiel J, Kuchna I, Nowicki K, Imaki H, Wegiel J, Marchi E, Ma SY, Chauhan A, Chauhan V, Bobrowicz TW, de Leon M, Louis LA, Cohen IL, London E, Brown WT, Wisniewski T (2010) The neuropathology of autism: defects of neurogenesis and neuronal migration, and dysplastic changes. Acta Neuropathol 119:755–770. CrossRef Medline

Xiao L, Chen D, Hu P, Wu J, Liu W, Zhao Y, Cao M, Fang Y, Bi W, Zheng Z, Ren J, Ji G, Wang Y, Yuan Z (2011) The c-Abl-MST1 signaling pathway mediates oxidative stress-induced neuronal cell death. J Neurosci 31:9611–9619. CrossRef Medline

Xie Z, Sanada K, Samuels BA, Shih H, Tsai LH (2003) Serine 732 phosphorylation of FAK by Cdk5 is important for microtubule organization, nuclear movement, and neuronal migration. Cell 114:469–482. CrossRef Medline

Ye T, Fu AKY, Ip NY (2012) Cyclin-dependent kinase 5 in axon growth and regeneration. In: International review of neurobiology (Jeffrey LG, Ephraim FT, eds), pp 91–115. San Diego: Academic.